

Supplementary Information

Superprotic Conductivity in $\text{RbH}_{2-3y}(\text{PO}_4)_{1-y}$: a Phosphate Deficient Analog to Cubic CsH_2PO_4 in the $(1-x)\text{RbH}_2\text{PO}_4 - x\text{Rb}_2\text{HPO}_4$ System

Grace Xiong, Louis S. Wang, and Sossina M. Haile

[Please note: This document was updated 5th December 2023, to give correct U_{iso} values in Table S4, and in Table S5 footnote]

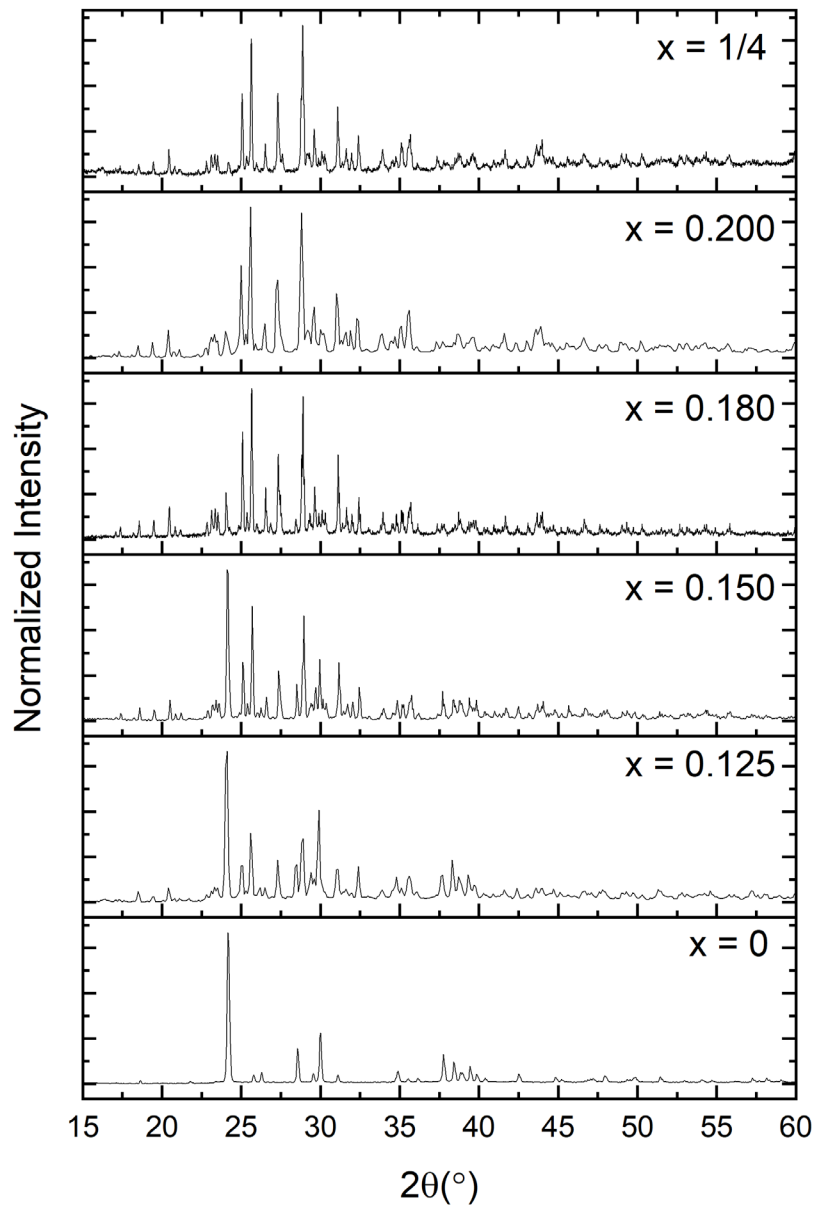


Figure S1. Diffraction patterns of materials in the $(1-x)$ RbH_2PO_4 – x Rb_2HPO_4 system (x as indicated) at temperatures just below the eutectoid reaction temperature and $p\text{H}_2\text{O} = 0.83$ atm. Measurement temperature is 235 °C, except for the $x = 1/4$ end-member ($\text{Rb}_5\text{H}_7(\text{PO}_4)_4$), which was measured at 237 °C. All patterns can be described as simple mixtures of RbH_2PO_4 (monoclinic)¹ and $\text{Rb}_5\text{H}_7(\text{PO}_4)_4$ ². Uncertainty in the composition is 0.003.

Table S1. Refined lattice parameters and phase fractions from high temperature x-ray diffraction measurements at $T = 235$ °C at specified values of x in $(1-x)$ $\text{RbH}_2\text{PO}_4 - x \text{ Rb}_2\text{HPO}_4$ materials. For $x = \frac{1}{4}$, the pattern was measured at 237 °C. Atomic coordinates and isotropic atomic displacement parameters of $\text{Rb}_5\text{H}_7(\text{PO}_4)_4$ and RbH_2PO_4 (m) were fixed at the values reported in studies by Averbuch-Pouchot et al.^{2,1} The cell parameters are found to be independent of the global composition, indicating the mutual insolubility of the two phases. The inconsistency between refined and expected phase fractions is attributed to challenges in obtaining truly random orientations of the crystallites in the composite samples, particularly because excessive grinding and pressing were avoided due to the tendency of the $\text{Rb}_5\text{H}_7(\text{PO}_4)_4$ phase to deliquesce under such treatment.

x	$\text{Rb}_5\text{H}_7(\text{PO}_4)_4$						RbH_2PO_4 (m) *					R_{wp} (%)	GOF
	a (Å)	b (Å)	c (Å)	Vol (Å ³)	Molar Fraction	Expected	a (Å)	b (Å)	c (Å)	β (°)	Vol (Å ³)		
0	--	--	--	--	0	0	9.559(1)	6.2544(3)	7.778(1)	108.960(3)	439.82(6)	8.43	10.09
0.125	28.577(4)	10.345(1)	6.1673(7)	1823.3(5)	0.197(3)	0.20	9.552(4)	6.2515(7)	7.782(3)	108.91(1)	439.6(1)	5.48	6.68
0.150	28.575(1)	10.3314(6)	6.1598(3)	1818.5(2)	0.308(3)	0.27	9.552(2)	6.2531(4)	7.777(1)	108.951(5)	439.41(6)	10.44	10.24
0.180	28.581(9)	10.3341(3)	6.1625(1)	1820.2(1)	0.731(4)	0.39	9.551(5)	6.2577(7)	7.794(3)	108.98(1)	440.54(6)	6.01	7.33
0.200	28.593(3)	10.335(1)	6.1626(6)	1821.2(5)	0.82(1)	0.50	9.53(1)	6.216(3)	7.81(1)	108.93(4)	438.0(2)	5.15	6.57
$\frac{1}{4}$	28.585(1)	10.3352(4)	6.1622(2)	1820.5(2)	1	1	--	--	--	--	--	6.00	5.25

*The refined molar fraction of RbH_2PO_4 (m) is simply $1 - (\text{refined molar phase fraction of } \text{Rb}_5\text{H}_7(\text{PO}_4)_4)$.

Table S2. Refined lattice parameters of $\text{RbH}_2\text{PO}_4(\text{m})$ from high temperature x-ray powder diffraction measurements of the single-phase material. Atomic coordinates and isotropic atomic displacement were fixed at the values reported by Averbuch-Pouchot et al.¹

Temperature (°C)	a (Å)	b (Å)	c (Å)	β (°)	Vol (Å³)	Rwp (%)	GooF
125	9.5950(5)	6.19098(8)	7.7270(3)	109.238(1)	433.37(1)	8.49	10.08
145	9.5923(5)	6.19916(8)	7.7351(3)	109.201(1)	434.37(1)	8.44	10.05
165	9.592(3)	6.2031(4)	7.746(2)	109.218(5)	435.26(9)	13.97	16.58
175	9.587(2)	6.2133(4)	7.747(1)	109.142(5)	436.00(8)	12.24	14.54
185	9.580(2)	6.2192(4)	7.756(1)	109.108(5)	436.69(8)	12.03	14.29
195	9.581(2)	6.2249(3)	7.761(1)	109.099(4)	437.41(6)	10.31	12.27
205	9.571(2)	6.2320(3)	7.760(1)	109.048(4)	437.58(6)	9.19	10.91
215	9.572(1)	6.2394(3)	7.767(1)	108.992(3)	438.66(6)	9.25	11.05
225	9.564(1)	6.2474(3)	7.774(1)	108.989(3)	439.29(6)	8.59	10.27
235	9.559(1)	6.2544(3)	7.778(1)	108.960(3)	439.82(6)	8.43	10.09
245	9.556(1)	6.2619(2)	7.787(1)	108.934(3)	440.81(5)	7.92	9.47
250	9.553(1)	6.2647(2)	7.787(1)	108.914(3)	440.88(5)	7.09	8.44

Table S3. Refined lattice parameters of $\text{Rb}_5\text{H}_7(\text{PO}_4)_4$ from high temperature x-ray powder diffraction measurements of the single-phase material. Atomic coordinates and isotropic atomic displacement parameters were fixed at the values reported by Averbuch-Pouchot et al.²

Temperature (°C)	a (Å)	b (Å)	c (Å)	Vol (Å ³)	Rwp (%)	GooF
65	28.4905(9)	10.2675(3)	6.0920(1)	1782.0(1)	4.97	4.34
155	28.546(1)	10.3025(4)	6.1266(2)	1801.8(2)	5.18	4.53
185	28.556(1)	10.3137(4)	6.1393(2)	1808.2(2)	5.45	4.77
237	28.585(1)	10.3352(4)	6.1622(2)	1820.5(2)	6.00	5.25
242	28.588(1)	10.3378(5)	6.1647(2)	1821.9(2)	5.80	5.07
245	28.589(1)	10.3391(6)	6.1663(3)	1822.7(2)	6.58	5.70

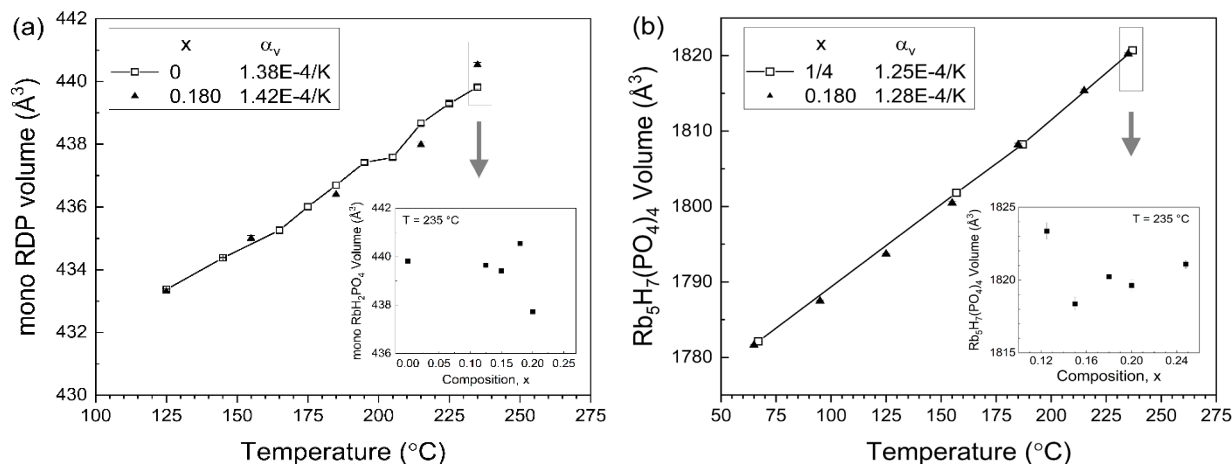


Figure S2. Comparison of volumes in single-phase and mixed phase systems of (a) monoclinic RbH_2PO_4 , and (b) orthorhombic $\text{Rb}_5\text{H}_7(\text{PO}_4)_4$ (as measured below the eutectoid temperature). At 125 °C and lower, monoclinic RbH_2PO_4 often occurred along with its tetragonal form; only the monoclinic results are reported here. The volumes of the phases are approximately independent of the global composition, x , in $(1-x)\text{RbH}_2\text{PO}_4 - x\text{Rb}_2\text{HPO}_4$ (see insets), indicating that RbH_2PO_4 and $\text{Rb}_5\text{H}_7(\text{PO}_4)_4$ remain stoichiometric, that is, they are mutually insoluble, up to the eutectoid temperature (242.0 ± 0.5 °C).

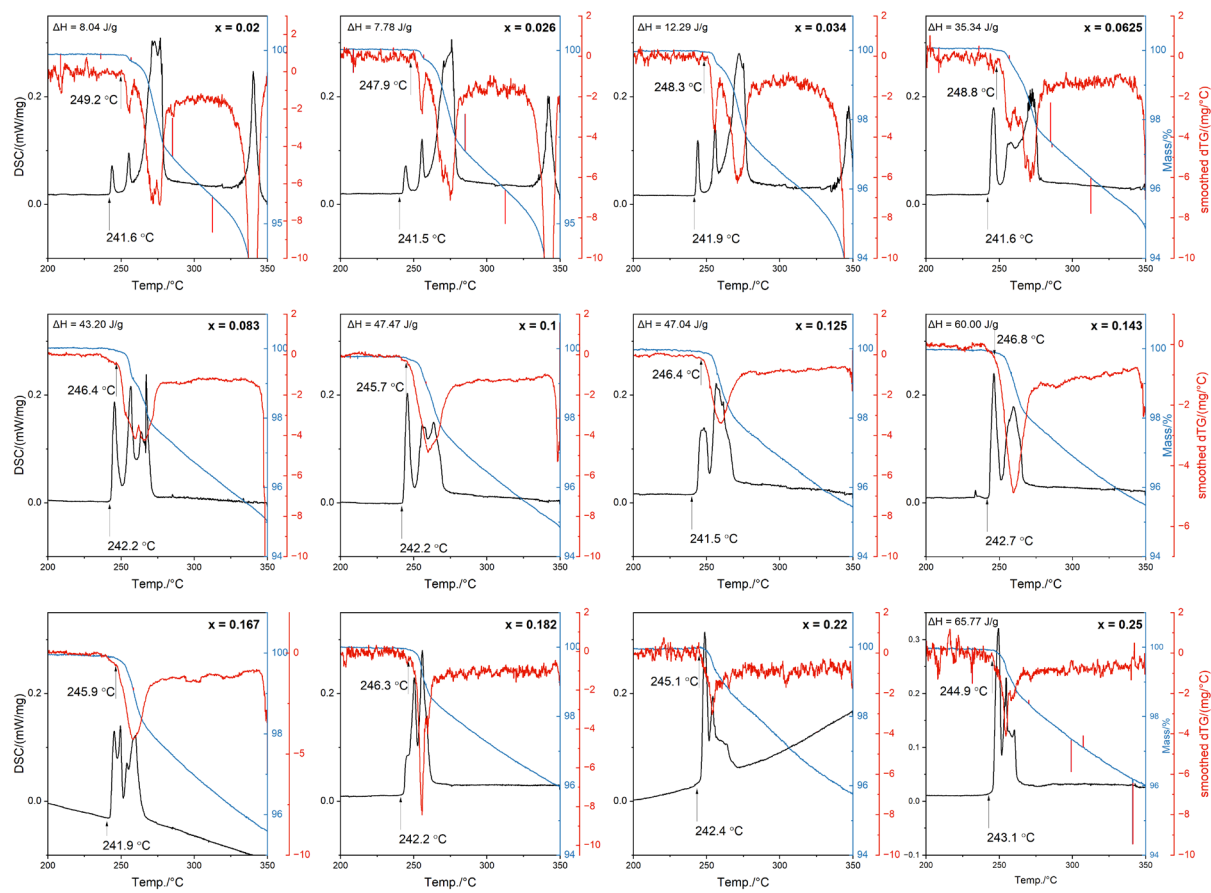


Figure S3. Simultaneous DSC/TGA measurement of materials in the $(1-x)$ $\text{RbH}_2\text{PO}_4 - x \text{Rb}_2\text{HPO}_4$ system at the compositions indicated and $p\text{H}_2\text{O} = 0.7$ atm; the composition $x = 0.22$ was measured with $p\text{H}_2\text{O} = 0.6$ atm. The average eutectoid phase transition temperature is 242.0°C with a standard deviation of 0.5°C . Dehydration at a slightly higher temperature occurs as a distinct thermal event for low x values and overlaps with the eutectoid transition at $x > 0.14$. At $x = \frac{1}{4}$, the end-member $\text{Rb}_5\text{H}_7(\text{PO}_4)_4$ undergoes a stoichiometric phase transition at a temperature just above that at which the eutectoid transformation occurs.

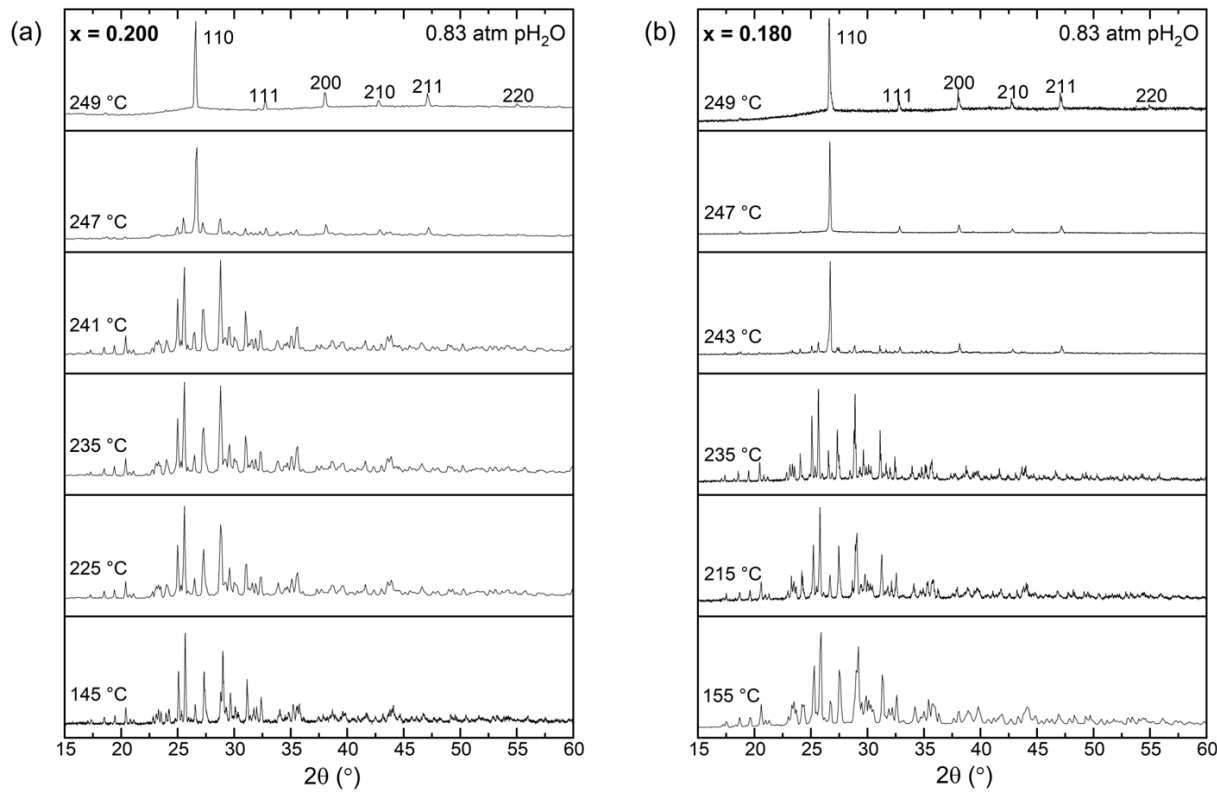


Figure S4. Diffraction patterns for (a) $x = 0.200$ and (b) $x = 0.180$ materials in the $(1-x)$ RbH₂PO₄ – x Rb₂HPO₄ system. At high temperature, the materials transform to a phase with simple cubic structure.

Table S4. Refined lattice parameters and phase fractions from high temperature x-ray diffraction analysis of composition $x = 0.200$ in the $(1-x)$ $\text{RbH}_2\text{PO}_4 - x \text{Rb}_2\text{HPO}_4$ system (Figure S4a). Atomic coordinates and isotropic atomic displacement parameters of $\text{Rb}_5\text{H}_7(\text{PO}_4)_4$ and $\text{RbH}_2\text{PO}_4(\text{m})$ were fixed at the values reported by Averbuch-Pouchot et al.^{2,1} The insensitivity of the refined molar fraction to temperature below the eutectoid transition, despite being larger than the expected value of 0.5, is consistent with mutual insolubility between $\text{Rb}_5\text{H}_7(\text{PO}_4)_4$ and RbH_2PO_4 (m).

Temperature (°C)	$\text{Rb}_5\text{H}_7(\text{PO}_4)_4$					RbH_2PO_4 (m)*					Rwp (%)	GooF
	a (Å)	b (Å)	c (Å)	Vol (Å ³)	Molar Fraction	a (Å)	b (Å)	c (Å)	β (°)	Vol (Å ³)		
145	28.536(2)	10.297(8)	6.128(5)	1801.0(4)	0.83(1)	9.58(3)	6.235(4)	7.72(2)	109.02(7)	436.5(3)	5.19	6.57
225	28.579(2)	10.3272(9)	6.1559(5)	1816.9(4)	0.80(1)	9.57(2)	6.238(2)	7.75(1)	109.03(4)	437.8(2)	5.01	6.37
235	28.593(3)	10.335(1)	6.1626(6)	1821.2(5)	0.82(1)	9.53(1)	6.216(3)	7.81(1)	108.93(4)	438.0(2)	5.15	6.57
241	28.590(2)	10.3340(9)	6.1630(5)	1820.8(4)	0.83(1)	9.56(2)	6.239(3)	7.75(1)	108.98(5)	438.04(3)	5.12	6.52

* The refined mole fraction of RbH_2PO_4 is simply $1 - (\text{refined molar phase fraction of } \text{Rb}_5\text{H}_7(\text{PO}_4)_4)$.

Temperature (°C)	$\text{Rb}_5\text{H}_7(\text{PO}_4)_4$					α -RDP (c)*					Crystallite Size (μm)	Rwp (%)	GooF			
	a (Å)	b (Å)	c (Å)	Vol (Å ³)	Molar Fraction	a (Å)	Vol (Å ³)	Oy	Oz	P-O dist. (Å)	Uiso Rb (Å ²)	Uiso P (Å ²)	Uiso O (Å ²)			
247	28.610(3)	10.353(1)	6.1742(6)	1828.9(3)	0.105(3)	4.702(1)	104.02(4)	0.204(2)	0.369(5)	1.51(5)	0.068(2)	0.054(4)	0.058(4)	0.151(8)	3.01	3.68
249					0	4.702(4)	103.95(3)	0.188(2)	0.402(6)	1.53(5)	0.068(2)	0.054(4)	0.058(4)	0.3(2)	2.28	2.98

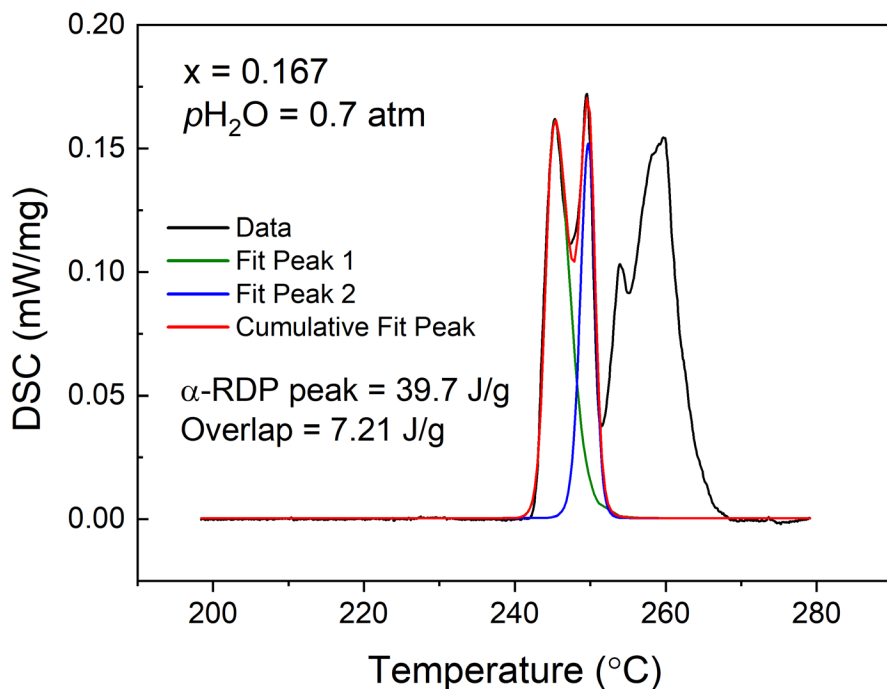
* The refined molar fraction of RbH_2PO_4 is simply $1 - (\text{refined molar phase fraction of } \text{Rb}_5\text{H}_7(\text{PO}_4)_4)$.

Table S5. Refined lattice parameters and phase fractions from high temperature x-ray diffraction analysis of composition $x = 0.180$ in the $(1-x)$ $\text{RbH}_2\text{PO}_4 - x \text{Rb}_2\text{HPO}_4$ system (Figure S4b).

Temperature (°C)	$\text{Rb}_5\text{H}_7(\text{PO}_4)_4$					RbH_2PO_4 (m)					α -RDP (c)*					P-O dist. (Å)	Molar Fraction	Crystallite Size (μm)	Rwp (%)	Goof	
	a (Å)	b (Å)	c (Å)	Vol (Å ³)	Molar Fraction	a (Å)	b (Å)	c (Å)	β (°)	Vol (Å ³)	Molar Fraction	a (Å)	Vol (Å ³)	Oy	Oz						
155	28.534(1)	10.2996(4)	6.1263(2)	1800.4(2)	0.687(5)	9.588(6)	6.1955(9)	7.750(3)	109.13(1)	435.00(8)	0.312(5)									7.84	9.46
185	28.556(1)	10.3133(4)	6.1396(2)	1808.1(2)	0.680(5)	9.5803(6)	6.2150(9)	7.752(3)	109.00(1)	436.41(8)	0.319(5)									7.77	9.40
215	28.571(1)	10.3252(4)	6.1535(2)	1815.3(2)	0.675(5)	9.563(6)	6.2363(8)	7.762(3)	108.90(1)	437.99(8)	0.324(5)									7.57	9.15
235	28.581(9)	10.3341(3)	6.1625(1)	1820.2(1)	0.731(4)	9.551(5)	6.2577(7)	7.794(3)	108.98(1)	440.54(6)	0.268(4)									6.01	7.33
243	28.584(2)	10.333(7)	6.1671(3)	1821.6(2)	0.072(2)	9.54(1)	6.263(2)	7.790(7)	108.99(2)	440.3(1)	0.0450(1)	4.7085(2)	104.38(1)	0.208(1)	0.376(3)	1.49(3)	0.882(2)	0.279(7)		6.59	8.02
245						9.51(1)	6.260(2)	7.78(1)	108.81(3)	439.2(1)	0.0301(1)	4.7096(1)	104.46(1)	0.203(1)	0.375(2)	1.51(2)	0.969(5)	0.292(6)		6.24	7.56
247												4.7130(1)	104.68(1)	0.211(1)	0.377(1)	1.46(1)		1.0322(5)		4.77	5.68
249												4.7183(3)	105.07(1)	0.184(1)	0.392(3)	1.57(2)		1.0222(6)		5.09	5.22

*The lattice parameters, phase fractions, and α -RDP crystallite size were allowed to vary freely. The displacement parameters obtained from the refinement of α -RDP at $x = 0.18$ and 245 °C (with values of 0.068(2) Å², 0.054(4) Å², and 0.058(4) Å² for Rb, P, and O, respectively, see main text) were employed as fixed inputs. The oxygen position was refined with a restraint targeting a P-O bond length of 1.53 Å.

.



$$\text{Asymmetric double sigmoidal curve: } y = y_0 + A \frac{\frac{1}{x-x_c+(w_1/2)}}{1+e^{\frac{x-x_c+(w_1/2)}{w_2}}} \left(1 - \frac{\frac{1}{x-x_c+(w_1/2)}}{1+e^{\frac{x-x_c+(w_1/2)}{w_2}}}\right)$$

Feature	Y_0	X_c	A	W_1	W_2	W_3
Peak 1	5e-4	245.54	0.22	2.8	0.53	1.16
Peak 2	5e-4	249.7	0.22	1.65	0.6	0.45

Figure S5. Illustration of the high degree of overlap between the thermal event associated with the eutectoid transition and that associated with dehydration in $(1-x) \text{ RbH}_2\text{PO}_4 - x \text{ Rb}_2\text{HPO}_4$ compositions with large x . Attempts to distinguish contributions from the individual processes via peak fitting (as shown above) to the overlapped response yielded unsatisfactory results.

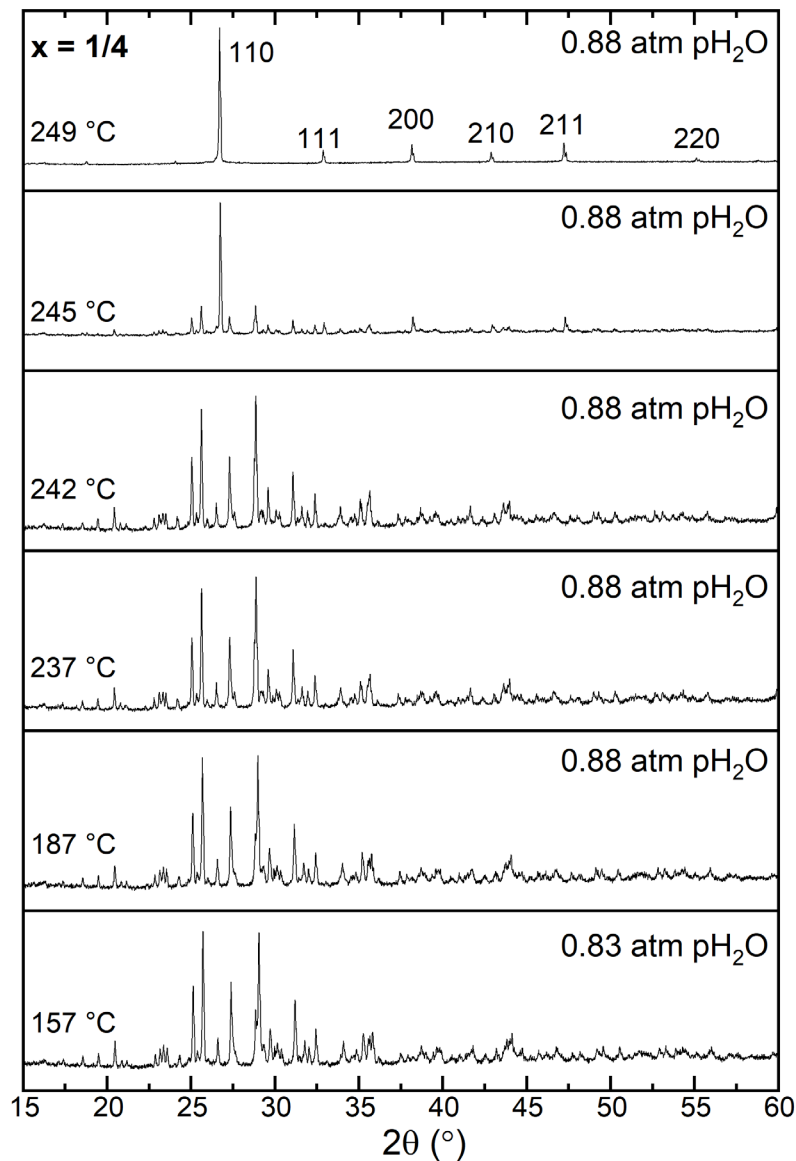


Figure S6. Diffraction patterns of $\text{Rb}_5\text{H}_7(\text{PO}_4)_4$ ($x = 1/4$ in the $(1-x)\text{RbH}_2\text{PO}_4 - x\text{Rb}_2\text{HPO}_4$ system) at the temperatures and steam partial pressures indicated. At high temperature, $\text{Rb}_5\text{H}_7(\text{PO}_4)_4$ transforms to a phase with a simple cubic lattice. Refinement results reported in Tables S3 and S6.

Table S6. Refined crystallographic properties of the α -RDP phase from high temperature x-ray diffraction patterns of $\text{Rb}_5\text{H}_7(\text{PO}_4)_4$ (Figure S6).

Temperature ($^\circ\text{C}$)	size (μm)	α -RDP (c)						Molar Fraction	Rwp%	Goof
		a (\AA)	Vol (\AA^3)	Oy	Oz	P-O distance				
245	0.98(6)	4.6945(1)	103.46(1)	0.195(1)	0.373(2)	1.54(2)	0.9801(2)	5.37	4.66	
249	0.27(2)	4.7026(1)	104.00(1)	0.187(1)	0.371(1)	1.58(2)	1	5.69	4.89	

At 249°C the material is fully transformed to α -RDP. At 245°C , a small amount of residual $\text{Rb}_5\text{H}_7(\text{PO}_4)_4$ remains, attributed to thermal gradients in the high temperature stage.

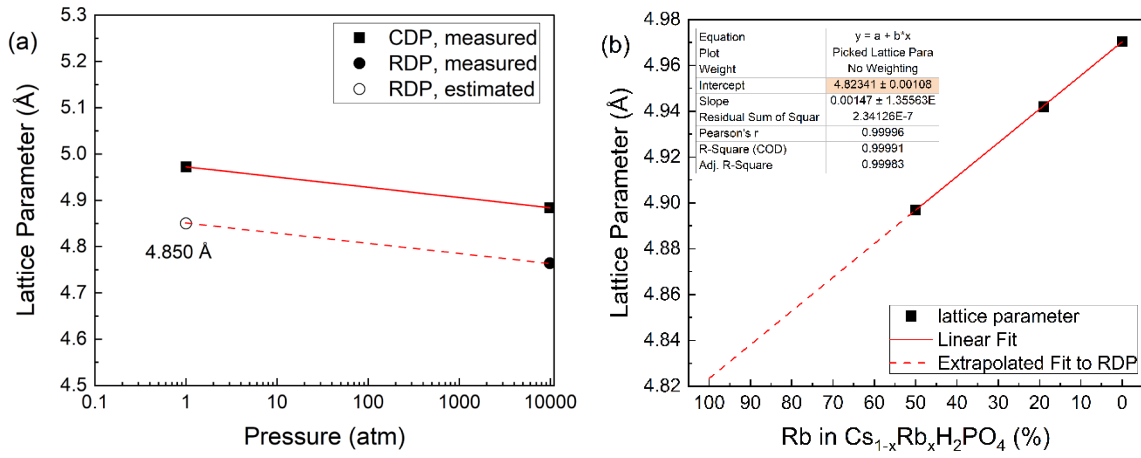


Figure S7. Estimation of the (hypothetical) lattice parameter of the cubic phase of RbH_2PO_4 at $249\text{ }^\circ\text{C}$ and 1 atm total pressure: (a) extrapolation from high pressure, assuming bulk modulus of CsH_2PO_4 ³ and (b) extrapolation from $\text{Cs}_{1-x}\text{Rb}_x\text{H}_2\text{PO}_4$ ⁴.

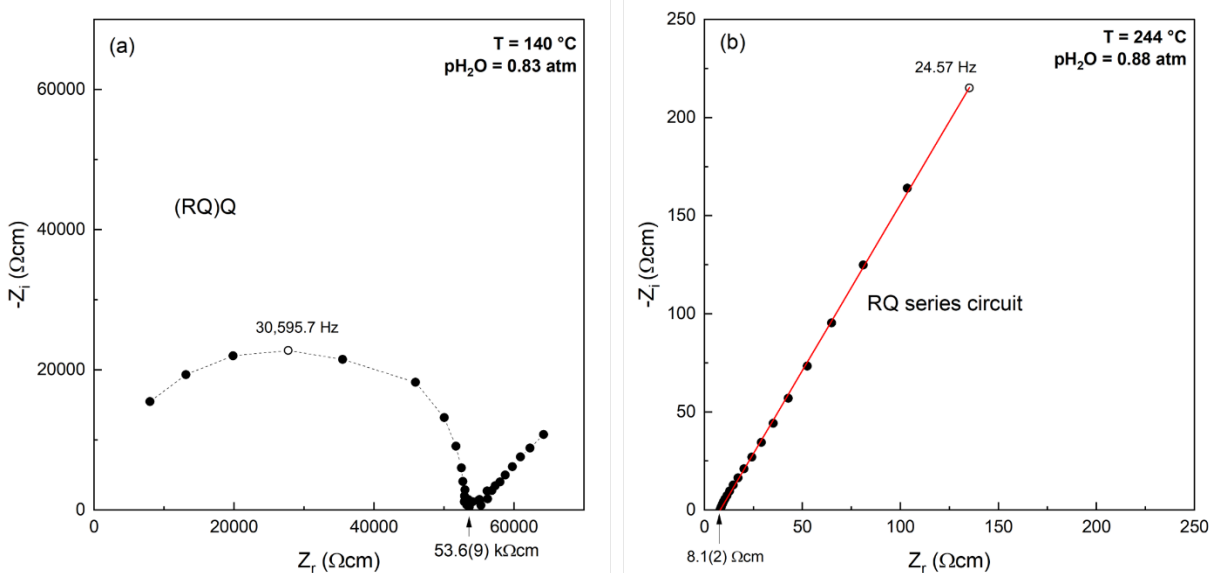


Figure S8. Selected impedance spectra collected from $\text{Rb}_{1+x}\text{H}_{2-x}\text{PO}_4$ at $x = 0.18$ (near the eutectoid composition) at the conditions indicated. In the (a) low conductivity regime the spectra are modeled using an (RQ)Q circuit, whereas in the (b) superprototypic phase, the impedance behavior is modeled using a resistor and a Warburg impedance element in series.

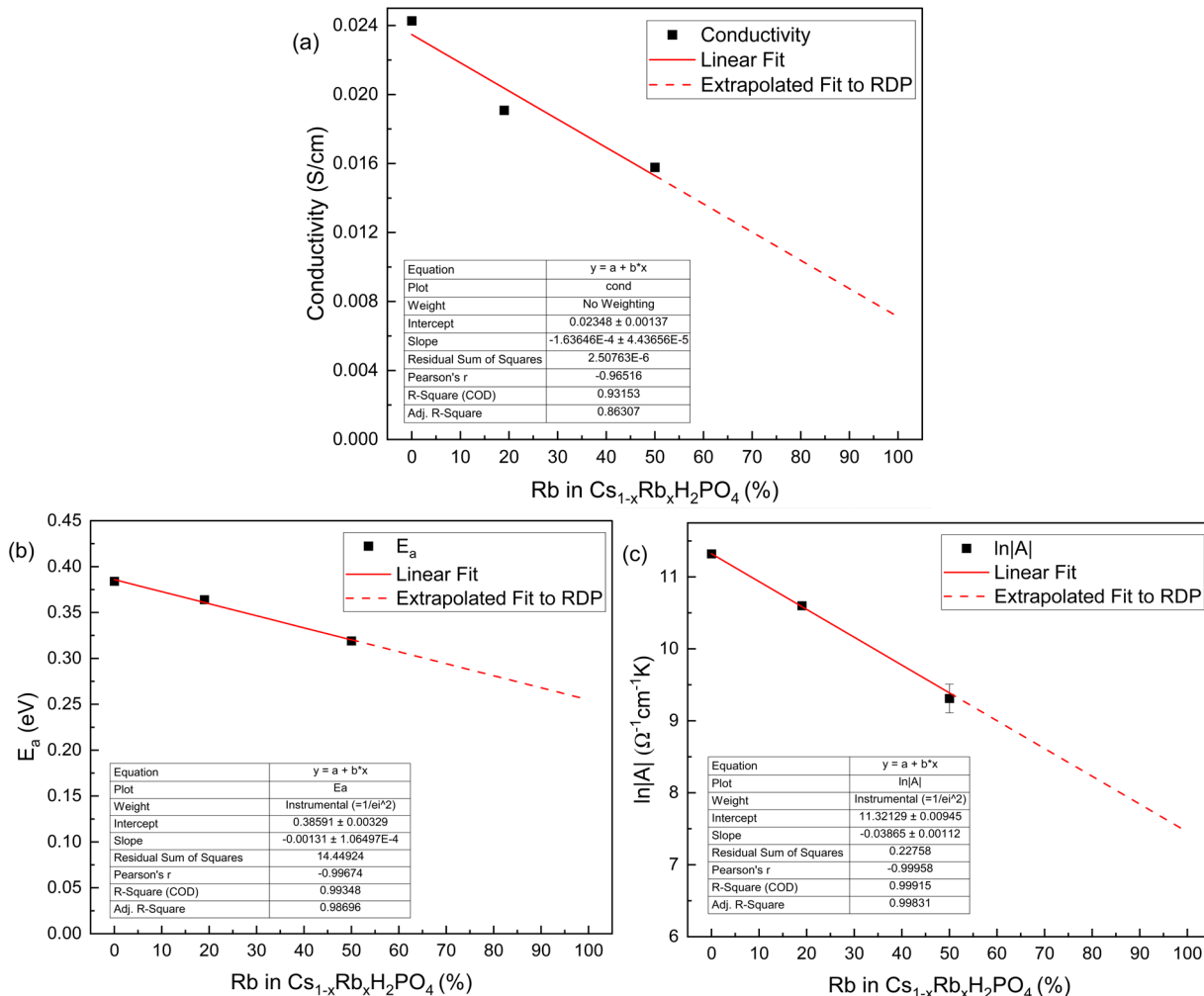


Figure S9. Estimation of (hypothetical) proton transport properties of the cubic RbH_2PO_4 . The (a) conductivity at 255 °C, (b) activation energy, and (c) preexponential factor were extrapolated from reported properties of $\text{Cs}_{1-x}\text{Rb}_x\text{H}_2\text{PO}_4$ ⁴. The extrapolations suggests that if stoichiometric RbH_2PO_4 occurred under ambient pressures, it would display an activation energy even smaller than that of stoichiometric CsH_2PO_4 , but its conductivity would be moderate due to a small value of the pre-exponential term. Studies of α -RDP compositions with more moderate nonstoichiometry than the eutectic composition would likely shed light on the trends in E_a and $\ln(A)$ on the overall conductivity.

References

1. M. T. Averbuch-Pouchot and A. Durif, *Acta Crystallographica*, 1985, **C41**, 665-667.
2. M. T. Averbuch-Pouchot and A. Durif, *Acta Crystallographica* 1985, **C41**, 1555–1556.
3. C. E. Botez, R. J. Tackett, J. D. Hermosillo, J. Z. Zhang, Y. S. Zhao and L. P. Wang, *Solid State Ionics*, 2012, **213**, 58-62.
4. A. Ikeda, D. A. Kitchev and S. M. Haile, *Journal of Materials Chemistry A*, 2014, **2**, 204-214.